HHS Public Access

Author manuscript

J Mater Chem B. Author manuscript; available in PMC 2019 October 07.

Published in final edited form as:

J Mater Chem B. 2018 October 7; 6(37): 5888–5895. doi:10.1039/C8TB01191E.

Delivery of mitoxantrone using a plant virus-based nanoparticle for the treatment of glioblastomas

Patricia Lam[a], **Richard Lin**[a], and **Nicole F. Steinmetz**[*,a,b,c]

[a.]Department of Biomedical Engineering, Case Western Reserve University, Cleveland, OH 44106, USA

[b.]Department of NanoEngineering, University of California, San Diego, La Jolla, CA 92093, USA

[c.]Moores Cancer Center, University of California, San Diego, La Jolla, CA 92093, USA

Abstract

Mitoxatrone (MTO), an antineoplastic chemotherapeutic, has potent activity against the most common and agressive type of primary brain tumor, glioblastoma multiforme (GBM). However, its poor penetration through the blood brain barrier, and cardiotoxic side effects from systemic delivery limit its effectiveness for clinical treatment. To address these limitations, we utilize a plant virus-based nanoparticle, cowpea mosaic virus (CPMV), to deliver MTO to treat GBM. In this work, we loaded MTO into the interior cavity of CPMV (CPMV-MTO) through diffusion through its pores. We report the uptake of CPMV-MTO in glioma cells and demonstrate its cytotoxic effects *in vitro* as a solo therapy, and in combination with tumor necrosis factor-related apoptosis-inducing ligand (TRAIL). These results reveal the potential for this plant virus-based nanoparticle platform for the treatment of GBM.

Graphical Abstract

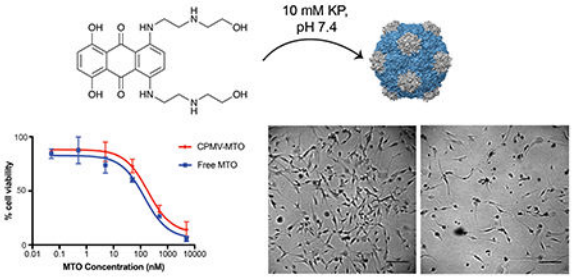

Introduction

Glioblastoma multiforme (GBM) is the most common and lethal primary malignancy of the brain. In the United States, approximately 10,000 cases are reported each year; the five-year survival rate is approximately 10%.[1] Current treatment for GBM includes surgery to remove

* nsteinmetz@ucsd.edu.

Conflicts of interest

There are no conflicts to declare.

the tumor, along with radiation therapy and chemotherapy. The poor prognosis is due to the aggressive nature of the tumor, and challenges associated with treatment, such as delivery of chemotherapeutics across the blood-brain barrier (BBB) and drug resistance.[2] Temozolomide (TMZ), an alkylating chemotherapeutic agent, is the standard drug for treatment of GBM,[3] however at least 50% of patients do not respond to TMZ.[4] Therefore, new chemotherapeutics have been explored to treat GBM. One such drug is mitoxantrone (MTO), a topoisomerase inhibitor that is also used in treatment of breast cancer, hepatic cancer, ovarian cancer, non-Hodgkin lymphoma, and leukemia.[5–7] Studies have shown that intratumoral injection of MTO is effective in improving survival of GBM patients,[6, 8–10] however less invasive treatments are more desirable. Systemic delivery of MTO is not feasible due to dose-limiting side effects such as cardiotoxicity, and poor penetration in brain tumors since MTO cannot cross the BBB.[11] Other studies have shown that intra-arterial transient cerebral hypoperfusion can deliver MTO to gliomas in *in vivo* models, but further research is required to assess therapeutic efficacy.[12]

To this end, nanoparticle-based delivery platforms are an attractive means to target therapeutic molecules to tumors and reduce systemic toxicities of chemotherapy regimens. Clinical trials are underway testing the use of synthetic nanoparticles that can pass through the BBB (i.e. liposomes, silica nanoparticles, gold nanoparticles, and iron oxide) for the treatment of GBM.[13]

An alternative to synthetic nanoparticles are biologics, such as virus-based nanoparticles. Various platforms derived from mammalian vectors as well as bacteriophages and plant viruses are being developed and tested.[14] Our laboratory focuses on the development of plant virus-based delivery strategies. In this work, we turned toward the cowpea mosaic virus (CPMV) as a tool for delivery of MTO to glioblastoma cells.

CPMV is a 30-nm icosahedral plant virus consisting of 60 copies each of a small and large protein, encapsulating a bipartite single-stranded RNA genome. CPMV has been broadly studied for biomedical applications, such as drug delivery,[15–18] imaging,[19, 20] and cancer vaccines.[21, 22] The propensity for CPMV to be taken up by many different cancer cells, such as HeLa (cervical cancer) and HT-29 (colon cancer) cell lines through its interactions with surface vimentin[23, 24] make it an attractive vehicle for delivery of chemotherapeutics. In the context of glioblastoma targeting and drug delivery, CPMV is an attractive candidate, because vimentin has been discussed as a potential marker for targeting GBM; vimentin expression is associated with a poor prognosis.[25] Furthermore, previous work using a mouse model of central nervous system (CNS) inflammation indicated that CPMV is rapidly internalized by cells of the BBB. CPMV particles target cerebral endothelial cells and breakdown of the BBB, as a result of the disease model, enabled movement of CPMV out of the vasculature into the brain parenchyma.[26]

We therefore investigate the use of CPMV for the delivery of MTO to treat GBM. We describe the loading of MTO inside the interior cavity of CPMV and report *in vitro* efficacy of CPMV-MTO nanoparticles in a model of GBM. Drug efficacy was evaluated as MTO solo therapy, free or CPMV delivered, and also assessed as combination approaches with

free MTO or CPMV-delivered MTO combined with TNF-related apoptosis inducing ligand (TRAIL), an immunotherapy known to synergize with MTO treatment in GBM.[27, 28]

Experimental

Materials and Methods

Propagation and purification of cowpea mosaic virus (CPMV).—CPMV was propagated by mechanical inoculation using 5-10 μg of CPMV per leaf of cowpea plants, California Blackeye No. 5 (*Vigna unguiculata*). Virus isolation was performed according to established protocols.[29] Empty CPMV (eCPMV) was obtained from Leaf Expression Systems (Norwich, UK).

Loading of mitoxantrone (MTO) into CPMV.—Mitoxantrone (MTO) dihydrochloride (Abcam) was dissolved in DMSO at a concentration of 50 mg mL^{-1}. A molar excess of 1250 MTO per mol CPMV was incubated with 4 mg CPMV in 10 mM potassium phosphate buffer, pH 7.4 at room temperature with gentle agitation overnight. Mitoxantrone-loaded CPMV (CPMV-MTO) was purified by ultracentrifugation at 150,000 × *g* for 1 hour over a 30% (w/v) sucrose cushion. The particle pellet was resuspended in 0.1 M potassium phosphate (KP) buffer, pH 7.0. CPMV-MTO particles were further purified using Zeba desalting columns (Thermo Scientific) to remove any excess MTO loosely bound to CPMV.

Bioconjugation of Oregon Green (OG) 488 to CPMV.—Oregon Green 488 Carboxylic Acid, Succinimidyl Ester was conjugated to the external lysine residues of CPMV through NHS chemistry. The reaction was performed by mixing 1200 molar excess of Oregon Green 488 Carboxylic Acid, Succinimidyl Ester (Thermo Scientific) with CPMV in 0.1 M potassium phosphate buffer, pH 7.0 containing 10% (v/v) DMSO. The reaction was allowed to proceed overnight with gentle agitation at room temperature. The reaction was purified with ultracentrifugation at 150,000 × *g* for 1 h over a 30% (w/v) sucrose cushion.

MTO release from CPMV-MTO.—CPMV-MTO (70 μL) was loaded into slide-a-lyzer mini dialysis units (Thermo Scientific) in triplicate. The dialysis units containing sample were placed on a float into 500 mL sodium phosphate buffer, pH 5.0 or 7.4, at room temperature. At various time points (0, 1, 3, 6, 12, 24, 48 and 72 hours), samples were removed and the amount of MTO per CPMV was determined by measuring the absorbance at 608 nm; the concentration of MTO-to-CPMV was calculated using the Beer Lambert law and the MTO and CPMV-specific extinction coefficients (see below).

UV/vis spectroscopy of CPMV-MTO, CPMV-OG, and CPMV-OG-MTO particles.—The concentrations of CPMV, Oregon Green 488 (OG), and MTO were determined by using the Beer-Lambert law using the following extinction coefficients: CPMV ε_{260}=8.1 mL mg^{-1} cm^{-1}, MW_{CPMV}=5.6 × 10^6 Da; OG ε_{496}=70,000 L mol^{-1} cm^{-1}; MTO ε_{608}=19,200 L mol^{-1} cm^{-1}.[30] Absorbance values were measured using UV-visible spectroscopy on a Nanodrop 2000 (Thermo Scientific).

Gel Electrophoresis.—For denaturing gel electrophoresis, samples were denatured by heating at 100° C for 10 minutes in NuPage 4× LDS Sample loading buffer (Thermo Fisher).

CPMV (10 μg) were loaded on 12% NuPage Bis-Tris protein gels (Thermo Fisher) and run in 1× MOPs buffer at 200V for 35 minutes. Gels were stained with Coomassie Blue. For native gel electrophoresis, 10 μg of sample was loaded into 0.8% (w/v) TAE agarose gels in 1× TAE buffer and run at 90V for 40 minutes. Gels were post-stained in 3× GelRed (Biotium) in water, and in Coomassie Blue. All gels were imaged on an AlphaImager HP or a FluorChem R (Protein Simple) and analyzed with Fiji.[31–33]

Transmission Electron Microscopy.—CPMV samples were diluted to 0.5-0.8 mg ml^{-1} in water and 20 μL was applied to glow-discharged carbon-coated 200 mesh grids for 2 minutes. Excess sample was blotted from the grids and the grids were rinsed twice with distilled water before staining with 2% (w/v) uranyl acetate for 2 minutes. Grids were imaged on a FEI Tecnai Spirit T12 transmission electron microscope operated at 200 kV.

Cell culture.—U87-MG cells (a human-derived glioblastoma cell line) were obtained from the ATCC (Manassas, VA). Cells were grown and maintained in Dulbecco's Modified Eagle's medium (DMEM, Cellgro) supplemented with 10% (v/v) fetal bovine serum (Atlanta Biologicals) and 1% (v/v) penicillin/streptomycin (Gibco). Cells were grown at 37°C in a 5% CO_2 humidified incubator.

Flow cytometry.—U87-MG cells were collected using enzyme-free Hank's cell dissociation buffer (Gibco) and resuspended to 2.5×10^6 cells mL^{-1}. Cells (5×10^5 cells in 0.2 mL) were added to 96-well V-bottom plates (Corning 3897). CPMV particles (1×10^5 particles per cell) were added in triplicate and incubated for 16 hours at 37°C in a 5% CO_2 humidified incubator. Following incubation, cells centrifuged at 500 x g and washed with FACS buffer (1mM EDTA, 1% (v/v) FBS, 25mM HEPES pH 7.0 in PBS) twice and fixed in 2% (v/v) paraformaldehyde in FACS buffer for 10 minutes. After fixing, cells were further washed in FACS buffer twice. Following washing, cells were resuspended in PBS and analyzed on a BD LSRII instrument. At least 10,000 gated events were recorded and data were analyzed using FlowJo 10.2 software.

Confocal microscopy.—U87-MG cells were seeded on circular coverslips in a 24 well suspension plate (25,000 cells in 500 μL). Cells were allowed to grow for 24 hours at 37°C in a 5% CO_2 humidified incubator before 1×10^7 particles per cell were added. Following incubation with particles for 24 hours, cells were washed three times with DPBS, then fixed in 5% (v/v) paraformaldehyde, 0.3% (v/v) glutaraldehyde in DPBS for 10 minutes. Cells were then washed three times with DPBS. Cellular components were stained as follows: (i) cell membranes were stained with wheat germ agglutinin, Alexa Fluor 555 conjugate (WGA-555; Invitrogen), 1:1000 in 5% (v/v) goat serum in DPBS; (ii) lysosomes were stained with an Alexa Fluor 488 anti-human LAMP-1 antibody (BioLegend), 1:500 in 5% (v/v) goat serum in DPBS); (iii) CPMV particles were stained with rabbit anti-CPMV antibody, 1:200 in 5% (v/v) goat serum in DPBS for 1 hour followed by goat anti-rabbit secondary antibody tagged with Alexa Fluor 647, 1:500 in 5% (v/v) goat serum in DPBS; (iv) nuclei were stained with DAPI found in the mounting medium. Cells were first stained with WGA-555, then permeabilized with 0.2% (v/v) Triton X-100 for 2 minutes and then blocked with 10% (v/v) goat serum in DPBS for 1 hour. Cells were washed three times with

DPBS in between treatments. Following all staining, coverslips were mounted onto slides with Fluoroshied with DAPI (Sigma-Aldrich) histology mounting medium and sealed with clear nail polish. Confocal images were obtained on a Leica TCS SPE confocal microscope with a 63× oil immersion objective. Images were analyzed with Fiji.[31–33]

Cell viability assay.—The cytotoxicity of free and CPMV-delivered MTO as solo or combination therapy with TRAIL was assessed with an MTT cell proliferation assay (ATCC). TNF-related apoptosis inducing ligand (TRAIL) was obtained from Enzo Lifesciences. 5000 U87-MG cells per well were seeded in treated black wall clear bottom 96-well plates (Corning 3603) for 24 hours. Then, MTO or CPMV-MTO was added in triplicate in varying concentrations (0.05, 0.5, 5, 50, 500, 5000 nM) for 24 hours. Medium containing treatments was removed and fresh media was added to the cells along with 50 ng ml^{-1} TRAIL (Enzo Lifesciences) and cells were further incubated for 24 hours. Following TRAIL treatment, 10 μL MTT reagent was added for 2-3 h before cells were lysed with 100 μL MTT detergent. Cells were incubated at room temperature overnight before being measured at 570 nm with a Tecan Infinite M Plex plate reader. Data were plotted and analyzed with GraphPad Prism 7 software.

Statistical Analysis.—Results are presented as means ± the standard deviation (SD). Statistical comparisons between groups were performed using a one-way ANOVA followed by the appropriate post hoc tests. Significance was accepted at p values <0.05.

Results and discussion

Formulation of MTO-loaded CPMV (CPMV-MTO)

Cowpea mosaic virus (CPMV) was purified from infected cowpea plants yielding 0.4-0.8 mg per 1 g of infected leaf material. It has previously been shown that fluorophores and therapeutics can be loaded into CPMV by infusion through its pores and RNA binding.[15, 34] MTO is a topoisomerase II inhibitor that binds to nucleic acid; it also carries a positive charge. Thus, we reasoned that infusion of MTO would be a suitable strategy for the formulation of CPMV-MTO. To achieving loading into the CPMV carrier, MTO was added to CPMV using a molar excess of 1250 MTO:CPMV followed by overnight incubation in 10 mM potassium phosphate (KP) buffer, pH 7.4 (Fig. 1A). While we typically store CPMV in 0.1 M KP buffer, we found that the lower salt concentration was necessary to keep MTO in solution. We tested higher and lower molar excess of MTO:CPMV; while ratios lower than 1250 MTO:CPMV yielded lower loading rates, using a larger molar excess did not result in greater drug loading, thus 1250 MTO per CPMV was used as the loading condition.

Purified CPMV-MTO maintained its structural integrity as indicated by transmission electron microscopy (Fig. 1B, C); icosahedral particles 30 nm in diameter were indistinguishable from native CPMV. UV-visible spectroscopy was used to assess the integrity of the particle after MTO loading and measure the amount of MTO loaded per CPMV (CPMV-MTO). Pure and intact particles have a A260 nm:A280 nm ratio of 1.7 ± 0.1. CPMV-MTO had a A260 nm:A280 nm ratio of 1.6. This is consistent with the TEM data indicating the particles remain intact. Based on the absorbance of MTO at 608 nm,[30] the amount of MTO per CPMV was determined, with loading of between 20-50 MTO

molecules per CPMV achieved (Fig. 1D). Size exclusion chromatography further confirmed that the CPMV particles are intact as their elution profiles matches native CPMV (not shown). Moreover, the elution profile indicates that MTO is indeed associated with CPMV as MTO (detected at 608 nm) co-elutes with CPMV (detected at 260 nm and 280 nm; Fig. 1E).

Further confirmation of MTO loading was achieved by native gel electrophoresis. After separation, gels were visualized under UV light after GelRed staining (Fig. 1F), red light (excitation 632 nm) (Fig. 1G), and with white light after staining with Coomassie Blue (Fig. 1H) to image the RNA, MTO, and protein components, respectively. Lane 1 shows native CPMV. This lane should only show signal under UV light (RNA) and white light (Coomassie-stained). Under red light, MTO can be detected (Fig. 1G), as seen in CPMV-MTO (lane 2) and in the MTO only sample (lane 4). Mitoxantrone has a net positive charge, so it runs towards to cathode (upwards in Figure 1), while CPMV particles migrate toward the anode (downwards in Figure 1) in agarose gel. The gel migration pattern indicates that MTO indeed co-migrates with the CPMV samples; the MTO signal under red light matches the GelRed and Coomassie stain. It should be noted that some amount of free MTO appears to be present for the CPMV-MTO samples. It is possible that this is an artifact of electrophoresis, i.e. that some drug is lost during the electrophoretic separation. Free drug was not detectable in size exclusion chromatography. Lastly to confirm whether MTO is indeed infused into CPMV via nucleic acid interactions or whether MTO may be associated with the CPMV proteins (either on the interior or exterior surface, we made use of empty CPMV particles (eCPMV). eCPMV are virus-like particles that do not contain its genomic RNA.[35] When eCPMV was infused with MTO using the same procedures as with CPMV, there was no detectable MTO associated with eCPMV based on UV-vis measurement (not shown) and agarose gel electrophoresis (Figure 1F). While the protein band for eCPMV is detectable after Coomassie staining, when exposed to UV and red light, no RNA or MTO band appeared (Figure 1F, lane 3). Together these data indicate that MTO is indeed loaded inside CPMV and that the loading mechanism is through its affinity to the RNA cargo.

Next, we evaluated the release profile of MTO from CPMV particles. CPMV-MTO particles were dialyzed against 0.1 M sodium phosphate buffer at pH 5.0 and 7.4. These conditions were selected to simulate the acidic environment of the lysosome, since this is where particles end up after being taken in by cells, and the body's physiological conditions. After 24 hours, about 50% of the MTO was released at pH 5.0, and release plateaued after that. Release at pH 7.4 was slower than that of pH 5.0, with release plateauing at 30-40% during the course of the study. Complete release was not seen after 72 hours for both pH conditions (Fig. 1I). The drug release study has limitations due to the simplicity of the drug release medium, and future studies using medium containing plasma can help improve *in vitro* release data. Nevertheless, while complete drug release under test tube conditions is not observed, we hypothesize that rapid clearance of CPMV will prevent extended release in the system and that complete release inside cells would be achieved due carrier degradation within the endolysosomal compartment (see also cell studies below).[36–38]

Synthesis and characterization of labeled CPMV

Oregon Green (OG) 488-labeled CPMV particles were prepared for cell uptake studies. Covalent conjugation of the OG fluorophores was achieved using established NHS-to-lysine chemistry. The conjugation of OG to CPMV was performed after MTO was loaded to avoid the possibility that surface bound OG would interfere with the pores of CPMV and prevent MTO infusion. Oregon Green 488 Carboxylic Acid, Succinimidyl Ester (OG) was reacted with CPMV or CPMV-MTO yielding CPMV-OG and CPMV-OG-MTO, respectively. Following conjugation and purification, the resulting CPMV-OG and CPMV-OG-MTO particles were characterized to confirm structural integrity and the degree of dye labeling. UV-visible spectroscopy was used to determine the degree of dye labeling and purity of particles. The degree of dye loading was 32 dyes/particle for CPMV-OG and 30 dyes/particle for CPMV-OG-MTO (Fig. 2A, B). Therefore, the MTO cargo inside CPMV does not interfere with the CPMV surface chemistry. Based on our previous studies focused on fluorescent CPMV particles, this degree of dye-loading is ideal to obtain good fluorescence signals, as increased dye intensity can lead to quenching of fluorescent signal.[37] Denaturing gel electrophoresis was performed to confirm successful conjugation of OG to CPMV. When separated on a denaturing gel, the small (24 kDa) and large (42 kDa) coat proteins of CPMV can be detected after Coomassie staining and visualization under white light; the small and large coat protein also show fluorescence as indicated by visualization under blue light (excitation 475 nm; lanes 2 and 3, Fig. 2C). This is consistent with addressable lysines being present on both coat protein subunits.[39]

Cellular uptake and subcellular localization of CPMV and CPMV-MTO

CPMV and CPMV-loaded with MTO were delivered to U87-MG cells, a human-derived glioblastoma cell line that is commonly used for glioma research. Previous research indicates that CPMV-mammalian cell uptake is mediated through binding to surface vimentin.[23] U87-MG cells also highly express vimentin,[40, 41] suggesting that they may interact with and internalize CPMV. Here, CPMV-U87-MG cell interactions were assessed using flow cytometry and confocal microscopy. For flow cytometry, we used OG-labeled CPMV and CPMV-MTO particles and analysis shows that CPMV-OG and CPMV-OG-MTO were both taken up by U87-MG cells (Fig. 3A), with the mean fluorescent intensity of CPMV-OG488 and CPMV-OG488-MTO both being statistically significant to the cells only control. Encapsulation of MTO into CPMV does not affect particle uptake into cells; this is as expected as MTO is loaded inside CPMV, therefore not altering the CPMV surface chemistry. Flow cytometry also indicated uptake of MTO with no statistically significant differences observed comparing free MTO vs. the CPMV-MTO formulation (Fig. 3B). Encapsulating MTO inside of CPMV did not to increase cellular uptake of the drug; this is as expected, because MTO is a cell permeable molecule. Based on our previous plant viral drug delivery studies,[42] we anticipate that benefits manifest *in vivo* based on favorable biodistribution of the CPMV-delivered MTO vs. free MTO, leading to increased MTO accumulation at the tumor site, therefore increasing the therapy effect while reducing systemic toxicity.

Confocal microscopy was performed in U87-MG cells treated with CPMV-MTO particles to confirm whether particles were indeed internalized into this cell line. Cells were stained with

Alexa Fluor 555-labeled wheat germ agglutinin (WGA-555) to mark the cell membrane, Alexa Fluor 488-labeled anti-human lysosome-associated membrane protein-1 (LAMP-1) antibody to indicate lysosomes, and 4',6-diamidino-2-phenylindole (DAPI) to stain the nucleus. CPMV-specific antibodies were used to detect CPMV. Confocal imaging data confirm that indeed CPMV was internalized into U87-MG cells and that the particles trafficked to the endolysosomal compartment as indicated by co-localization with LAMP-1 marker (Fig. 3H-L). Localization of CPMV in the lysosomes is consistent with previous reports in which immune and cancer cells were studies.[40, 43–45] Our previous studies indicate that the protein carrier is degraded inside the endolysosome;[37] therefore we expect drug release upon cell entry; in particular the labile RNA is expected to be degraded quickly under the harsh conditions of the endolysosome, leading to complete release of MTO from its CPMV carrier. Because MTO is a cell permeable drug, it is expected that it will cross the membranes to reach its target, the nuclear DNA.

Cytotoxicity of encapsulated and free mitoxantrone

The cytotoxicity of free and CPMV-encapsulated MTO in U87-MG cells was assessed using an MTT assay. Because most therapies are ineffective as solo therapies, we also explored the combination of MTO/CPMV-MTO with the immunotherapy TRAIL. Tumor necrosis factor-related apoptosis-inducing ligand (TRAIL) has been recognized as an attractive cancer therapy, largely because of its specificity to cancer cells with little to no effect on healthy cells that do not express the TRAIL death receptors (DR4 and DR5).[46] In glioblastoma however, TRAIL as a solo therapy has not seen much success, largely due to the fact that glioblastomas (including U87-MG) cells are largely resistant to TRAIL.[47] Combination with chemotherapy regimes, however, can sensitize cancer cells to TRAIL, and it has been shown that MTO is a TRAIL sensitizing agent.[27] For these reasons we evaluated MTO/CPMV-MTO as solo and TRAIL combination therapies.

A gradient of MTO concentrations ranging from 0.05 nM to 5000 nM were added to cells for 24 hours. CPMV only was added as a control. Following incubation with MTO/CPMV-MTO fresh media were added to cells and they were incubated for another 24 hours before assessing cytotoxicity. In the case of combination therapy, TRAIL at 50 ng ml^{-1} was added and cells and incubated for 24 hours before assessing cytotoxicity. As shown in Figure 4A, CPMV particles by themselves and TRAIL are not cytotoxic. Over three biological replicates, the same trend was found (Fig. 4B). With TRAIL treatment, the IC50 values for free mitoxantrone decreased from 212.8±88.3 nM to 65.9±20.2 nM. The CPMV-encapsulated mitoxantrone showed IC50 values similar to that of free drug (269.0±70.2 nM and 153.1±83.1 nM with TRAIL). These results suggest that CPMV-MTO is therapeutically active and that combination of MTO or CPMV/MTO+TRAIL is more potent compared to either solo therapy. Cell death was further confirmed through bright field imaging of U87-MG cells (Fig. 4C). Cells were imaged at 0, 24, 48, and 72 hours after treatment with free MTO, CPMV-MTO and CPMV only. Over time, cells continued to proliferate in the cells only and CPMV only treatments. However, with free MTO and CPMV-MTO treatment, there were less cells visible and changes in cell morphology, indicating cell death.

While *in vitro* studies do not show increased efficacy of the CPMV-delivered drug, we hypothesize that the nanoparticle delivery approach would confer advantages *in vivo*. In fact, most nanoparticle-assisted drug delivery approaches do not increase efficacy, but rather render the treatment safer. One of the major side effects of systemic MTO administration is cardiotoxicity, leading to heart failure.[48] Nanoparticles alter the biodistribution of drugs, and in the case of CPMV, it was shown that CPMV does not accumulate in the heart.[38] Therefore, CPMV-delivered MTO may be a suitable strategy for delivery of this chemotherapy, evading deposition of the drug in the heart and thus reducing its systemic toxicities.

Conclusions

In this work, we have developed a novel plant-based viral nanoparticle using cowpea mosaic virus. Currently, delivery of therapeutics, such as the anti-cancer drug mitoxantrone, is hampered by poor delivery to the target site and unwanted side effects due to systemic delivery. To overcome these technological hurdles, we encapsulated mitoxantrone into CPMV, a particle that is biocompatible and non-infectious towards mammals. From our *in vitro* studies, using flow cytometry, confocal microscopy and cell viability assays, we have shown there is uptake of CPMV-MTO in U87-MG glioblastoma cells, and that encapsulated mitoxantrone retains its therapeutic efficacy. These results lead to potential future applications for plant virus nanotechnology to treat glioblastomas.

Acknowledgements

This work was funded by a Research Scholar Award from the American Cancer Society (RSG-15-144-01-CDD) to N.F.S. and a NIH Training grant (T32EB007509) to R.L. We thank Neetu Gulati, Sudheer Molugu, and the Cleveland Center for Membrane and Structural Biology for assistance with TEM.

Notes and references

1. Ostrom QT, Gittleman H, Fulop J, Liu M, Blanda R, Kromer C, Wolinsky Y, Kruchko C and Barnholtz-Sloan JS, Neuro Oncol, 2015, 17 Suppl 4, iv1–iv62. [PubMed: 26511214]
2. Kim SS, Harford JB, Pirollo KF and Chang EH, Biochem Biophys Res Commun, 2015, 468, 485–489. [PubMed: 26116770]
3. Newlands ES, Blackledge GR, Slack JA, Rustin GJ, Smith DB, Stuart NS, Quarterman CP, Hoffman R, Stevens MF, Brampton MH and et al., Br J Cancer, 1992, 65, 287–291. [PubMed: 1739631]
4. Lee SY, Genes & Diseases, 2016, 3, 198–210. [PubMed: 30258889]
5. Senkal M, Tonn JC, Schonmayr R, Schachenmayr W, Eickhoff U, Kemen M and Kollig E, J Neurooncol, 1997, 32, 203–208. [PubMed: 9049881]
6. DiMeco F, Li KW, Tyler BM, Wolf AS, Brem H and Olivi A, J Neurosurg, 2002, 97, 1173–1178. [PubMed: 12450040]
7. Boiardi A, Salmaggi A, Pozzi A, Broggi G and Silvani A, J Neurooncol, 1996, 27, 157–162. [PubMed: 8699238]
8. Boiardi A, Eoli M, Pozzi A, Salmaggi A, Broggi G and Silvani A, Ital J Neurol Sci, 1999, 20, 43–48. [PubMed: 10933484]
9. Boiardi A, Bartolomei M, Silvani A, Eoli M, Salmaggi A, Lamperti E, Milanesi I, Botturi A, Rocca P, Bodei L, Broggi G and Paganelli G, J Neurooncol, 2005, 72, 125–131. [PubMed: 15925992]
10. Saini M, Roser F, Hussein S, Samii M and Bellinzona M, J Neurooncol, 2004, 68, 225–232. [PubMed: 15332325]

11. Dobson JM, Hohenhaus AE and Peaston AE, in Small Animal Clinical Pharmacology (Second Edition), eds. Page SW and Church DB, W.B. Saunders, Edinburgh, 2008, pp. 330–366.
12. Ellis JA, Cooke J, Singh-Moon RP, Wang M, Bruce JN, Emala CW, Bigio IJ and Joshi S, J Neurooncol, 2016, 130, 449–454. [PubMed: 27576697]
13. Shergalis A, Bankhead A, 3rd, Luesakul U, Muangsin N and Neamati N, Pharmacol Rev, 2018, 70, 412–445. [PubMed: 29669750]
14. Wen AM and Steinmetz NF, Chemical Society Reviews, 2016, 45, 4074–4126. [PubMed: 27152673]
15. Yildiz I, Lee KL, Chen K, Shukla S and Steinmetz NF, Journal of controlled release : official journal of the Controlled Release Society, 2013, 172, 568–578. [PubMed: 23665254]
16. Aljabali AA, Shukla S, Lomonossoff GP, Steinmetz NF and Evans DJ, Mol Pharm, 2013, 10, 3–10. [PubMed: 22827473]
17. Wen AM, Lee KL, Cao P, Pangilinan K, Carpenter BL, Lam P, Veliz FA, Ghiladi RA, Advincula RC and Steinmetz NF, Bioconjug Chem, 2016, 27, 1227–1235. [PubMed: 27077475]
18. Ganguly R, Wen AM, Myer AB, Czech T, Sahu S, Steinmetz NF and Raman P, Nanoscale, 2016, 8, 6542–6554. [PubMed: 26935414]
19. Wen AM, Shukla S, Saxena P, Aljabali AAA, Yildiz I, Dey S, Mealy JE, Yang AC, Evans DJ, Lomonossoff GP and Steinmetz NF, Biomacromolecules, 2012, 13, 3990–4001. [PubMed: 23121655]
20. Wu C, Barnhill H, Liang X, Wang Q and Jiang H, Optics Communications, 2005, 255, 366–374.
21. Lizotte PH, Wen AM, Sheen MR, Fields J, Rojanasopondist P, Steinmetz NF and Fiering S, Nat Nano, 2016, 11, 295–303.
22. Shukla S, Myers JT, Woods SE, Gong X, Czapar AE, Commandeur U, Huang AY, Levine AD and Steinmetz NF, Biomaterials, 2017, 121, 15–27. [PubMed: 28063980]
23. Koudelka KJ, Destito G, Plummer EM, Trauger SA, Siuzdak G and Manchester M, PLoS pathogens, 2009, 5, e1000417. [PubMed: 19412526]
24. Koudelka KJ, Rae CS, Gonzalez MJ and Manchester M, J Virol, 2007, 81, 1632–1640. [PubMed: 17121801]
25. Zhao J, Zhang L, Dong X, Liu L, Huo L and Chen H, Appl Immunohistochem Mol Morphol, 2016, DOI: 10.1097/PAI.0000000000000420.
26. Shriver LP, Koudelka KJ and Manchester M, J Neuroimmunol, 2009, 211, 66–72. [PubMed: 19394707]
27. Senbabaoglu F, Cingoz A, Kaya E, Kazancioglu S, Lack NA, Acilan C and Bagci-Onder T, Cancer Biology & Therapy, 2016, 17, 546–557. [PubMed: 27029345]
28. Grandhi TS, Potta T, Taylor DJ, Tian Y, Johnson RH, Meldrum DR and Rege K, Nanomedicine (Lond), 2014, 9, 1775–1788. [PubMed: 24195660]
29. Wellink J, Methods Mol Biol, 1998, 81, 205–209. [PubMed: 9760508]
30. Bell DH, Biochimica et biophysica acta, 1988, 949, 132–137. [PubMed: 3334848]
31. Schindelin J, Arganda-Carreras I, Frise E, Kaynig V, Longair M, Pietzsch T, Preibisch S, Rueden C, Saalfeld S, Schmid B, Tinevez J-Y, White DJ, Hartenstein V, Eliceiri K, Tomancak P and Cardona A, Nat Meth, 2012, 9, 676–682.
32. Schindelin J, Rueden CT, Hiner MC and Eliceiri KW, Molecular reproduction and development, 2015, 82, 518–529. [PubMed: 26153368]
33. Schneider CA, Rasband WS and Eliceiri KW, Nature methods, 2012, 9, 671–675. [PubMed: 22930834]
34. Wen AM, Le N, Zhou X, Steinmetz NF and Popkin DL, ACS Biomater Sci Eng, 2015, 1, 1050–1054. [PubMed: 27280157]
35. Saunders K, Sainsbury F and Lomonossoff GP, Virology, 2009, 393, 329–337. [PubMed: 19733890]
36. Leong HS, Steinmetz NF, Ablack A, Destito G, Zijlstra A, Stuhlmann H, Manchester M and Lewis JD, Nat Protoc, 2010, 5, 1406–1417. [PubMed: 20671724]
37. Wen AM, Infusino M, De Luca A, Kernan DL, Czapar AE, Strangi G and Steinmetz NF, Bioconjugate Chem, 2015, 26, 51–62.

38. Singh P, Prasuhn D, Yeh RM, Destito G, Rae CS, Osborn K, Finn MG and Manchester M, Journal of Controlled Release, 2007, 120, 41–50. [PubMed: 17512998]
39. Chatterji A, Ochoa WF, Paine M, Ratna BR, Johnson JE and Lin T, Chem Biol, 2004, 11, 855–863. [PubMed: 15217618]
40. Trog D, Fountoulakis M, Friedlein A and Golubnitschaja O, Proteomics, 2006, 6, 2924–2930. [PubMed: 16596702]
41. Trog D, Yeghiazaryan K, Schild HH and Golubnitschaja O, Amino acids, 2008, 34, 539–545. [PubMed: 18046501]
42. Czapar AE, Zheng Y-R, Riddell IA, Shukla S, Awuah SG, Lippard SJ and Steinmetz NF, ACS Nano, 2016, 10, 4119–4126. [PubMed: 26982250]
43. Gonzalez MJ, Plummer EM, Rae CS and Manchester M, PLoS One, 2009, 4, e7981. [PubMed: 19956734]
44. Wu Z, Chen K, Yildiz I, Dirksen A, Fischer R, Dawson PE and Steinmetz NF, Nanoscale, 2012, 4, 3567–3576. [PubMed: 22508503]
45. Plummer EM and Manchester M, Mol. Pharmaceutics, 2013, 10, 26–32.
46. Wiley SR, Schooley K, Smolak PJ, Din WS, Huang CP, Nicholl JK, Sutherland GR, Smith TD, Rauch C, Smith CA and et al., Immunity, 1995, 3, 673–682. [PubMed: 8777713]
47. Puduvalli VK, Sampath D, Bruner JM, Nangia J, Xu R and Kyritsis AP, Apoptosis, 2005, 10, 233–243. [PubMed: 15711939]
48. Faulds D, Balfour JA, Chrisp P and Langtry HD, Drugs, 1991, 41, 400–449. [PubMed: 1711446]

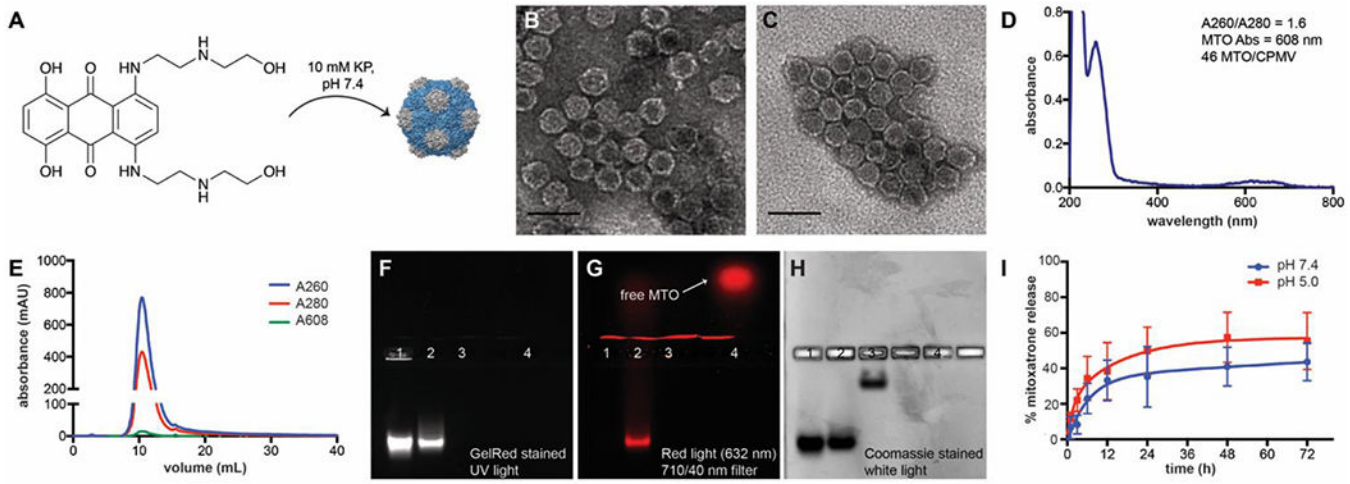

Figure 1.

Characterization of CPMV-MTO particles. (A) Structure of mitoxantrone (MTO) and the loading scheme into CPMV particles. (B, C) TEM of CPMV and CPMV-MTO; scale bar = 100 nm. (D) UV-Visible spectroscopy spectra of CPMV-MTO. An A260:A280 ratio of 1.7 +/− 0.1 indicates that the particles are intact. (E) Size exclusion chromatography of CPMV-MTO. Mitoxantrone (A608) co-elutes with the particle (A260 for RNA, A280 for protein). (F-H) Native gel electrophoresis under 3 different lights indicating loading of MTO into CPMV via interactions with its RNA. Under UV light and gel staining with GelRed, RNA is visible (F); under red light, mitoxantrone appears in red (G). There are empty lanes surrounding lane 4 due to the strong fluorescence signal of MTO to prevent diffusion to sample lanes. There is red signal above all the lanes that is an artifact of imaging. Free mitoxantrone is indicated by the arrow above lane 4; under white light, Coomassie stained protein bands are visible (H). Lane 1=native CPMV; lane 2=CPMV-MTO; lane 3=eCPMV-MTO; lane 4=free MTO. (I) MTO release of CPMV-MTO over a 72-hour time course in sodium phosphate buffer, pH 5.0 (red) and 7.4 (blue) at room temperature.

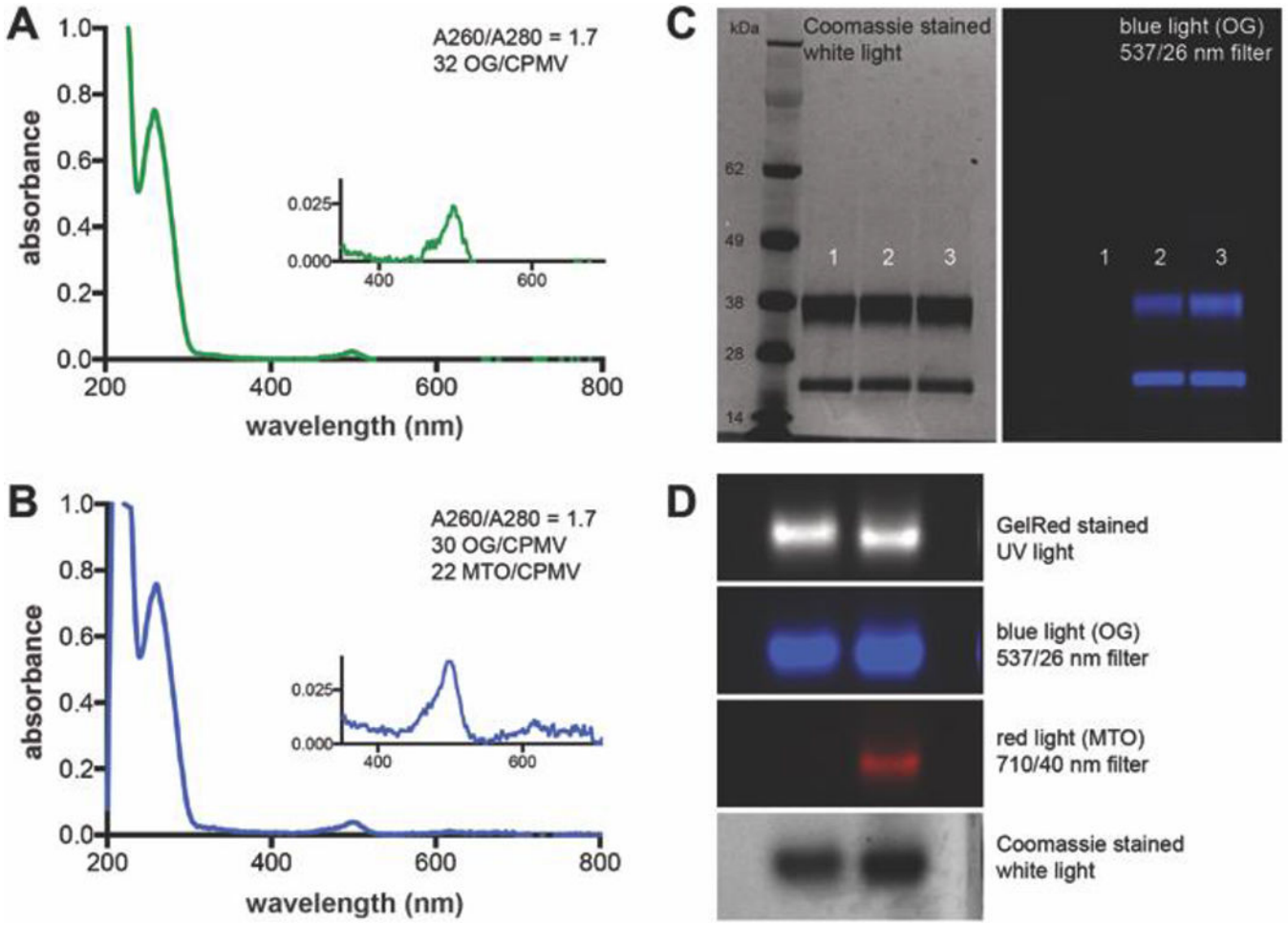

Figure 2.

Characterization of CPMV-OG-MTO. Oregon Green (OG) 488 NHS ester was conjugated to CPMV via reaction with surface exposed lysine residues. (A-B) UV-visible spectroscopy of CPMV-OG (A), and CPMV-OG-MTO (B), with the inset showing the peak for the OG/MTO. (C) SDS-PAGE of CPMV-OG and CPMV-OG-MTO showing attachment of OG with CPMV. Left gel is Coomassie stained and visualized under white light. Right gel is visualized under blue left before staining. Lane 1=native CPMV; lane 2=CPMV-OG; lane 3=CPMV-OG-MTO. (D) Native agarose gel under different wavelength of light showing attachment of OG and loading of MTO into CPMV. Left lane=CPMV-OG; right lane=CPMV-OG-MTO.

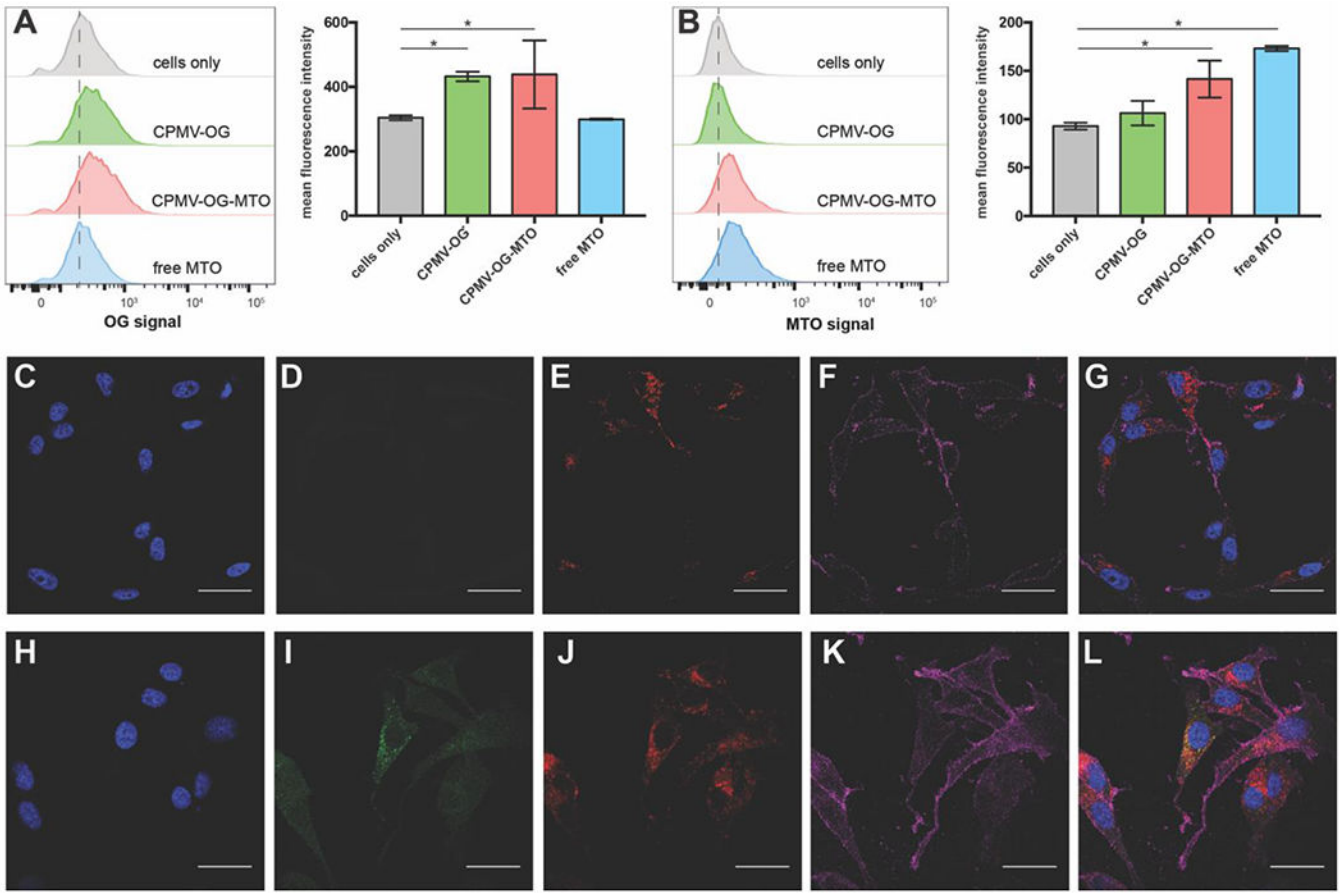

Figure 3.

Uptake of free mitoxantrone (MTO) and encapsulated MTO (CPMV-MTO) in U87-MG cells. (A-B) Uptake of CPMV (A) and MTO (B) was measured by flow cytometry; histograms and the mean fluorescence intensities are plotted. Statistical significance was measured using a one-way ANOVA and Dunnett's multiple comparisons test (*$p<0.05$, n=3). (C-L) Confocal microscopy showing U87-MG cells only (C-G) and U87-MG cells after exposure to CPMV-OG-MTO (H-L). The nucleus is labeled with DAPI (blue) (C, H), CPMV particles are shown in green (imaged based on the OG label) (D, I), lysosomes are stained with anti-LAMP-1 antibody (red) (E, J) and the cell membrane is labeled with wheat germ agglutinin (magenta) (F, K). Merged images of are shown in panels G and L. Scale bar = 25 μm.

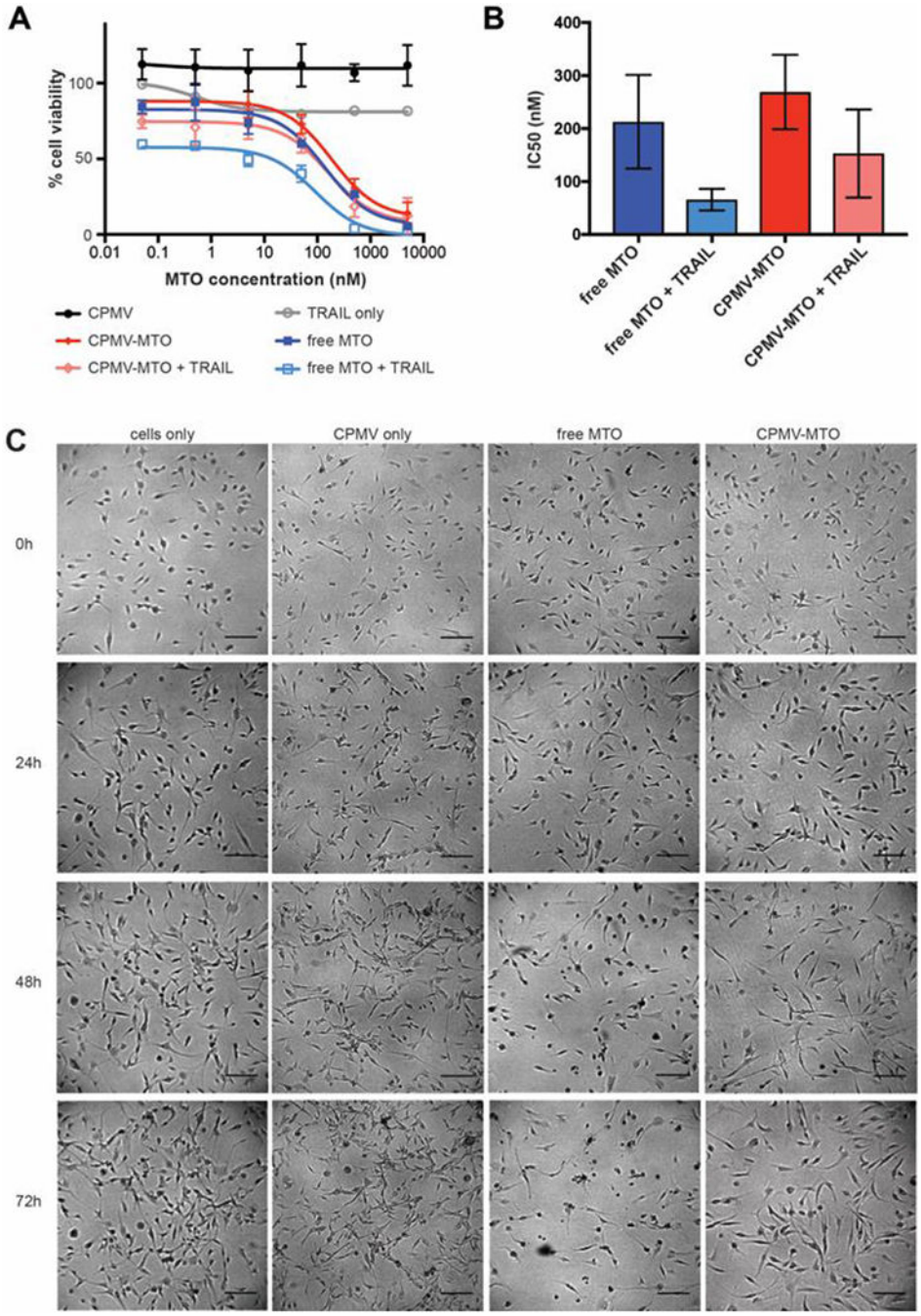

Figure 4.

(A) Cell viability of U87-MG cells following mitoxantrone (MTO) and combination of MTO and TRAIL treatment; MTO was delivered as free MTO or encapsulated CPMV-MTO. The combination therapy of MTO and TRAIL was more efficacious in all formulations. Data plotted are an average of 3 technical replicates. Representative data from 3 biological replicates are shown. (B) Relative IC50 values comparing all the drug treatments. Data are an average of 3 biological replicates ± SD. (C) U87-MG cells were imaged with bright field microscopy before and after addition of 100 nM free MTO or CPMV-MTO at 24h, 48h and

72h. The equivalent amount of CPMV was added as a control. Images are representative of 3 biological replicates. Scale bar = 200 μm